COMPUTER RESEARCH AND MODELING
2025 VOL. 16 NO. 5 P. e1107–e1123
DOI: 10.20537/2076-7633-2025-16-5-1107-1123

Ки&М

NUMERICAL METHODS AND THE BASIS FOR THEIR APPLICATION

UDC: 519.876.5

Computation of a shock wave structure in a gas mixture based on the Boltzmann equation with accuracy control

S. S. Sitnikov[1,2,a], F. G. Tcheremissine[3]

[1]Moscow Institute of Physics and Technology,
9 Institutskiy per., Dolgoprudny, Moscow Region, 141701, Russia
[2]National Research Center "Kurchatov Institute",
1 Akademika Kurchatova pl., Moscow, 123182, Russia
[3]Federal Research Center "Computer Science and Control" of the Russian Academy of Sciences,
44 Vavilov st., 119333 Moscow, Russia

E-mail: [a] mailtosergeysitnikov@yandex.ru

Received 29.02.2024, after completion — 23.08.2024.
Accepted for publication 30.08.2024.

In this paper, the structure of a shock wave in a binary gas mixture is studied on the basis of direct solution of the Boltzmann kinetic equation. The conservative projection method is used to evaluate the collision integral in the kinetic equation. The applied evaluation formulas and numerical methods are described in detail. The model of hard spheres is used as an interaction potential of molecules. Numerical simulation is performed using the developed simulation environment software, which makes it possible to study both steady and non-steady flows of gas mixtures in various flow regimes and for an arbitrary geometry of the problem. Modeling is performed on a cluster architecture. Due to the use of code parallelization technologies, a significant acceleration of computations is achieved. With a fixed accuracy controlled by the simulation parameters, the distributions of macroscopic characteristics of the mixture components through the shock wave front were obtained. Computations were conducted for various ratios of molecular masses and Mach numbers. The total accuracy of at least 1 % for the local values of molecular density and temperature and 3 % for the shock front width was achieved. The obtained results were compared with existing computation data. The results presented in this paper are of theoretical significance, and can serve as a test computation, since they are obtained using the exact Boltzmann equation.

Keywords: rarefied gas dynamics, binary gas mixtures, Boltzmann kinetic equation, projection method, numerical simulation, shock wave structure

Citation: *Computer Research and Modeling*, 2025, vol. 16, no. 5, pp. e1107–e1123.

The results of the work were obtained using computational resources of MCC NRC "Kurchatov Institute" (http://computing.nrcki.ru/).

КОМПЬЮТЕРНЫЕ ИССЛЕДОВАНИЯ
И МОДЕЛИРОВАНИЕ 2025 Т. 16 № 5 С. e1107–e1123
DOI: 10.20537/2076-7633-2025-16-5-1107-1123

Ки&М

ЧИСЛЕННЫЕ МЕТОДЫ И ОСНОВЫ ИХ РЕАЛИЗАЦИИ

УДК: 519.876.5

Расчет структуры ударной волны в газовой смеси на основе уравнения Больцмана с контролем точности

С. С. Ситников[1,2,a], Ф. Г. Черемисин[3]

[1]Московский физико-технический институт (национальный исследовательский университет),
Россия, 141701, Московская область, г. Долгопрудный, Институтский переулок, д. 9
[2]Национальный исследовательский центр «Курчатовский институт»,
Россия, 123182, г. Москва, пл. Академика Курчатова, д. 1
[3]Федеральный исследовательский центр «Информатика и управление» Российской академии наук,
Россия, 119333, г. Москва, ул. Вавилова, д. 44

E-mail: [a] mailtosergeysitnikov@yandex.ru

Получено 29.02.2024, после доработки — 23.08.2024.
Принято к публикации 30.08.2024.

В работе проведено исследование структуры ударной волны в бинарной газовой смеси на основе прямого решения кинетического уравнения Больцмана. Для вычисления интеграла столкновений в кинетическом уравнении используется консервативный проекционный метод. Детально описаны применяемые расчетные формулы и методика вычислений. В качестве потенциала взаимодействия молекул используется модель твердых сфер. Численное моделирование проводится с использованием разработанной программно-моделирующей среды, которая позволяет исследовать стационарные и нестационарные течения газовых смесей в различных режимах и для произвольной геометрии задачи. Моделирование выполняется на системе кластерной архитектуры. За счет использования технологий распараллеливания кода достигается значительное ускорение вычислений. С фиксированной точностью, контролируемой параметрами моделирования, получены распределения макроскопических величин компонентов смеси по фронту ударной волны. Расчеты выполнены для различных соотношений молекулярных масс и чисел Маха. Достигнута общая точность моделирования не менее 1 % по локальным значениям концентрации и температуры и 3 % по ширине фронта ударной волны. Проведено сравнение полученных результатов с существующими расчетными данными. Представленные в данной работе результаты имеют теоретическое значение, а также могут служить в качестве тестового расчета, поскольку они получены с использованием точного уравнения Больцмана.

Ключевые слова: динамика разреженных газов, бинарные газовые смеси, кинетическое уравнение Больцмана, проекционный метод, численное моделирование, структура ударной волны

Результаты работы получены с использованием вычислительных ресурсов ОВК НИЦ «Курчатовский институт» (http://computing.nrcki.ru/).

Introduction

The study of shock waves in rarefied gases is of importance for aerodynamics [Wu et al., 2013], satellites and spacecraft development [Cao, White, Kontis, 2021], microflow device design [Gospodinov, Roussinov, Dankov, 2014] and other fields of science and technology [Sharipov, Dias, 2017; Kloss et al., 2011]. Besides, obtaining the structure of a shock wave is one of the key classical problems in kinetic theory [Dodulad, Tcheremissine, 2013; Raines, 2002]. In this paper, an approach to numerical simulation of shock waves in rarefied gas mixtures is proposed.

With respect to gas rarefaction, hydrodynamic, transitional and free molecular flow regimes are usually distinguished. In hydrodynamic regime, the Navier – Stokes (N-S) equations can be used to simulate gas flows. However, as the mean free path increases, the N-S equations become invalid in the transitional and free molecular flow regimes. In the indicated regimes, the gas flows are often studied using model kinetic equations [Xu, 2021] or the Direct Simulation Monte Carlo (DSMC) method [Bird, 2013]. However, both of these approaches have known limitations in applicability and accuracy of simulation [Sharipov, Seleznev, 1998].

In our work, the simulation is performed on the basis of direct solution of the Boltzmann kinetic equation, which describes the gas flow in all regimes and is suitable for studying processes occurring in a shock wave in a gas on a scale of the order of the mean free path of molecules. However, numerical solution of the Boltzmann equation is a complex computational problem due to the presence of a multidimensional nonlinear collision integral on its right side. To calculate the collision integrals, we use the conservative projection method (CPM) proposed in [Черемисин, 1997; Черемисин, 2000]. The CPM conserves energy, momentum, and mass and ensures that the collision integral from the Maxwell distribution function is exactly equal to zero [Черемисин, 2000]. The computational complexity of the method is quite acceptable for numerical simulation.

In this paper, the structure of a plane shock wave in a binary gas mixture is studied. Modeling is performed for various ratios of molecular masses of the mixture components and Mach numbers using the developed simulation environment software. Computations are performed on a cluster architecture system. Significant acceleration of computations is achieved due to the use of code parallelization technologies. Special attention is paid to simulation accuracy control, as well as verification of the obtained results.

Theoretical basis

Consider the N-component gas mixture. We introduce the distribution functions of the mixture components: $f_i(t, \mathbf{r}, \mathbf{p})$, $i = \overline{1, N}$. Macroscopic quantities describing the state of each component are expressed through its distribution function:
molecular density

$$n_i(t, \mathbf{r}) = \int\limits_{R^3} f_i \, d^3 p, \tag{1}$$

hydrodynamic velocity

$$\mathbf{u}_i(t, \mathbf{r}) = \frac{1}{n_i m_i} \int\limits_{R^3} \mathbf{p}_i f_i \, d^3 p, \tag{2}$$

temperature

$$T_i(t, \mathbf{r}) = \frac{1}{3 k_B n_i m_i} \int\limits_{R^3} (\mathbf{p}_i - m_i \mathbf{u}_i)^2 f_i \, d^3 p. \tag{3}$$

Here $\mathbf{p}_i$ and m_i are momentum and mass of molecules of the i-th component of the mixture respectively, and k_B is the Boltzmann constant. Molecular density, hydrodynamic velocity and

temperature of the entire mixture are expressed through the corresponding macroscopic quantities of the components as follows:

$$n = \sum_{i=1}^{N} n_i, \quad \mathbf{u} = \frac{1}{n}\sum_{i=1}^{N} n_i \mathbf{u}_i, \quad T = \frac{1}{n}\sum_{i=1}^{N} n_i T_i. \tag{4}$$

The evolution of the distribution functions of the mixture components over time is determined by the Boltzmann kinetic equation [Коган, 1967], which for the case of the N-component gas mixture can be written as the following system

$$\frac{\partial f_i}{\partial t} + \frac{\mathbf{p}_i}{m_i}\frac{\partial f_i}{\partial \mathbf{r}} = \sum_j I_{ij}, \quad i,\ j = \overline{1,\ N}. \tag{5}$$

Here $I_{ij} = I_{ij}(t, \mathbf{r}, \mathbf{p}_i)$ are the collision integrals for the interaction of the i-th and j-th components,

$$I_{ij}(t, \mathbf{r}, \mathbf{p}_i) = \int_0^{2\pi} d\varphi \int_0^{b_{\max}} b\, db \int_{\mathbb{R}^3} d^3 p_j (f_i' f_j' - f_i f_j) g_{ij}. \tag{6}$$

In the expression for the collision integrals (6), $f_i = f_i(t, \mathbf{r}, \mathbf{p}_i)$, $f_j = f_j(t, \mathbf{r}, \mathbf{p}_j)$, $f_i' = f_i(t, \mathbf{r}, \mathbf{p}_i')$, $f_j' = f_j(t, \mathbf{r}, \mathbf{p}_j')$, $\mathbf{p}_i$ и $\mathbf{p}_j$ are initial momenta of two colliding molecules, $g = \left|\frac{\mathbf{p}_i}{m_i} - \frac{\mathbf{p}_j}{m_j}\right|$ is their relative velocity, b is an impact parameter, $b_{\max}$ is the cut-off radius of the interaction potential, φ is an azimuth angle, $\mathbf{p}_i'$ and $\mathbf{p}_j'$ are the molecular momenta after collision, determined from the initial momenta $\mathbf{p}_i$ and $\mathbf{p}_j$ and collision parameters b, φ using a given molecular interaction potential $U(\mathbf{r})$.

In this work, the model of hard spheres is used as the interaction potential of molecules

$$U(\mathbf{r}) = \begin{cases} \infty, & r < d_{ij}, \\ 0, & r \geqslant d_{ij}. \end{cases} \tag{7}$$

Here $d_{ij} = \frac{d_i + d_j}{2}$, d_i and d_j are the diameters of molecules of the i-th and j-th components, respectively [Hirschfelder, Curtiss, Bird, 1954]. The scattering angle of molecules for a given interaction potential depends only on the impact parameter

$$\theta(b) = 2\arccos\left(\frac{b}{d_{ij}}\right). \tag{8}$$

Hereinafter, the dimensionless variables are used. We number the components of the gas mixture in descending order of molecular masses. Let the characteristic parameters m_0, d_0 be equal to those of the first component of the gas mixture, $n_0 = \sum\limits_i n_i$, $i = \overline{1,\ N}$, and T_0 be initial temperature of the mixture (ahead of the shock wave). We define the characteristic velocity, time and mean free path of molecules

$$v_0 = \sqrt{\frac{T_0}{m_0}}, \quad \tau = \frac{\lambda}{v_0}, \quad \lambda = \frac{1}{\sqrt{2}\pi n_0 d_0^2}. \tag{9}$$

We make the transition to dimensionless variables according to the following scheme:

$$f \to \frac{f}{n_0 (m_0 v_0)^{-3}}, \quad t \to \frac{t}{\tau}, \quad \mathbf{p} \to \frac{\mathbf{p}}{m_0 v_0}, \quad m \to \frac{m}{m_0}, \quad \mathbf{r} \to \frac{\mathbf{r}}{\lambda}, \quad b \to \frac{b}{d_0}, \quad d \to \frac{d}{d_0}, \quad g \to \frac{g}{v_0}.$$

In dimensionless variables, the system (5) takes the form

$$\frac{\partial f_i}{\partial t} + \frac{\mathbf{p}_i}{m_i}\frac{\partial f_i}{\partial \mathbf{r}} = \frac{1}{\sqrt{2}\pi}\sum_j I_{ij}, \quad i,\ j = \overline{1,\ N}, \tag{10}$$

where the collision integral has the form

$$I_{ij} = \int_0^{2\pi} d\varphi \int_0^{d_{ij}} b\,db \int_{R^3} d^3 p_j (f_i' f_j' - f_i f_j) g_{ij}. \tag{11}$$

We will further use the system of Boltzmann equations, written in the form (10), to simulate the flow of a binary gas mixture.

Transition from mathematical model to numerical simulation

For the numerical solution of system (10) the method of splitting by physical processes [Aristov, Cheremisin, 1980] is applied. At each iterative time step, the advection equations are first solved

$$\frac{\partial f_i}{\partial t} + \frac{\mathbf{p}_i}{m_i}\frac{\partial f_i}{\partial \mathbf{r}} = 0, \quad i = \overline{1,\ N}, \tag{12}$$

and then the obtained intermediate values are used as initial conditions for the relaxation equations

$$\frac{\partial f_i}{\partial t} = \frac{1}{\sqrt{2}\pi}\sum_j I_{ij}, \quad i,\ j = \overline{1,\ N}. \tag{13}$$

Equations (13) are solved by splitting into a sequence of equations

$$\frac{\partial f_i}{\partial t} = \frac{1}{\sqrt{2}\pi} I_{ii}, \quad i = \overline{1,\ N}, \tag{14}$$

$$\frac{\partial f_i}{\partial t} = \frac{1}{\sqrt{2}\pi}\sum_{j\neq i} I_{ij}, \quad i,\ j = \overline{1,\ N}. \tag{15}$$

Here, equations (14) describe intracomponent collisions of molecules, and equations (15) describe intercomponent collisions. Equations (15) are split into the sequence of equations

$$\frac{\partial f_i}{\partial t} = \frac{1}{\sqrt{2}\pi} I_{ij}, \quad i,\ j = \overline{1,\ N}, \quad j \neq i. \tag{16}$$

Thus, solving of system (10) is reduced to the sequential solving of systems (12), (14) and (16) at each time step.

Solving the relaxation equations using the conservative projection method

The key problem is the solution of relaxation equations (14) and (16). In our work, a conservative projection method [Черемисин, 1997; Черемисин, 2000] is used for this purpose. This method conserves energy, momentum and mass and ensures that the collision integral from the Maxwell distribution function is exactly equal to zero.

Since the conservative projection method is the basis of this work, we will briefly explain its essence. The value of the collision integral at some point $\mathbf{p}_{i_\gamma}$ can be written using the Dirac delta function

$$I_{ij}\left(\mathbf{p}_{i_\gamma}\right) = \int\limits_{R^3} I_{ij}(\mathbf{p}_i)\delta\left(\mathbf{p}_i - \mathbf{p}_{i_\gamma}\right) d^3p_i = \int\limits_0^{2\pi} d\varphi \int\limits_0^{d_{ij}} b\,db \int\limits_{R^3} d^3p_j \int\limits_{R^3} d^3p_i (f_i' f_j' - f_i f_j) g_{ij} \delta\left(\mathbf{p}_i - \mathbf{p}_{i_\gamma}\right). \quad (17)$$

We perform the change of variables $\mathbf{p}_i \leftrightarrow \mathbf{p}_i'$, $\mathbf{p}_j \leftrightarrow \mathbf{p}_j'$ and then take into account the equalities $g_{ij}' = g_{ij}$, $d^3p_i' d^3p_j' = d^3p_i d^3p_j$

$$I_{ij}\left(\mathbf{p}_{i_\gamma}\right) = \frac{1}{2}\int\limits_0^{2\pi} d\varphi \int\limits_0^{d_{ij}} b\,db \int\limits_{R^3} d^3p_j \int\limits_{R^3} d^3p_i \left\{(f_i' f_j' - f_i f_j) g_{ij} \left(\delta\left(\mathbf{p}_i - \mathbf{p}_{i_\gamma}\right) - \delta\left(\mathbf{p}_i' - \mathbf{p}_{i_\gamma}\right)\right)\right\}. \quad (18)$$

For the i-th component of the gas mixture, we construct a uniform grid in the momentum space, enclosed in a sphere Ω_i of radius large enough so that the values of the distribution functions outside this sphere can be considered negligibly small. Let V_{0i}, N_{0i} be volume of the sphere and number of momentum nodes $S_i = \{\mathbf{p}_\gamma\}$ in it, respectively. Here $V_{0i} = N_{0i}\Delta V$, where $\Delta V = (\Delta p)^3$ is a volume per node of the momentum grid, Δp is the momentum grid step that is the same for all components of the mixture.

As initial momenta $\mathbf{p}_i$, $\mathbf{p}_j$, we take any pair of the grid nodes $\mathbf{p}_{\alpha_\nu}$, $\mathbf{p}_{\beta_\nu}$, respectively. Since post-collision momenta do not coincide with the grid nodes, they are decomposed with the same weight coefficient r_ν over two pairs of grid nodes, selected from the eight nodes closest to them

$$\mathbf{p}_i' = (1 - r_\nu)\mathbf{p}_{\lambda_\nu} + r_\nu \mathbf{p}_{\lambda_\nu + s_\nu}, \quad \mathbf{p}_j' = (1 - r_\nu)\mathbf{p}_{\mu_\nu} + r_\nu \mathbf{p}_{\mu_\nu - s_\nu}. \quad (19)$$

Here s_ν is the three-dimensional vector of displacement to the neighboring grid node, which components can take values equal to 0, ±1. The coefficient r_ν is found from the energy conservation condition

$$\frac{\mathbf{p}_i'^2}{2m_i} + \frac{\mathbf{p}_j'^2}{2m_j} = (1 - r_\nu)\left(\frac{\mathbf{p}_{\lambda_\nu}^2}{2m_i} + \frac{\mathbf{p}_{\mu_\nu}^2}{2m_j}\right) + r_\nu\left(\frac{\mathbf{p}_{\lambda_\nu + s_\nu}^2}{2m_i} + \frac{\mathbf{p}_{\lambda_\nu - s_\nu}^2}{2m_j}\right). \quad (20)$$

For the product of the distribution functions at post-collision momenta, we use exponential interpolation

$$f_i' f_j' \equiv f_i(\mathbf{p}_i') f_j(\mathbf{p}_j') = \left(f_i\left(\mathbf{p}_{\lambda_\nu}\right) f_j\left(\mathbf{p}_{\mu_\nu}\right)\right)^{1-r_\nu} \left(f_i\left(\mathbf{p}_{\lambda_\nu + s_\nu}\right) f_j\left(\mathbf{p}_{\mu_\nu - s_\nu}\right)\right)^{r_\nu}. \quad (21)$$

For calculation of (18) we move from integration over b to integration over $\sigma = \frac{b^2}{\left(\frac{d_i + d_j}{2}\right)^2}$ and apply a uniform 8-dimensional cubature Korobov grid [Коробов, 1989] of N_ν nodes $\mathbf{p}_{\alpha_\nu}$, $\mathbf{p}_{\beta_\nu}$, φ, σ in domain $\Omega_i \times \Omega_j \times [0, 2\pi) \times [0, 1)$. At each iterative time step, a new Korobov grid is used, obtained by periodically shifting by a random vector. The random shift vector does not change the integration domain.

Finally, we obtain the following formulas for the collision integral, in which only the grid nodes are used:

$$I_{ij}\left(\mathbf{p}_{i_\gamma}\right) = B_{ij} \sum_{\nu=1}^{N_\nu} \left[-\delta_{i_\gamma,\alpha_\nu} + (1 - r_\nu)\delta_{i_\gamma,\lambda_\nu} + r_\nu \delta_{i_\gamma,\lambda_\nu + s_\nu}\right] \Delta_\nu^{ij}, \quad (22)$$

where $\delta_{\alpha,\beta}$ is the Kronecker delta,

$$B_{ij} = \frac{\pi\left(\frac{d_i+d_j}{2}\right)^2 N_{0i} V_{0j}}{2N_\nu}$$

and

$$\Delta_\nu^{ij} = \left\{ f_i\left(\mathbf{p}_{\alpha_\nu}\right) f_j\left(\mathbf{p}_{\beta_\nu}\right) - \left(f_i\left(\mathbf{p}_{\lambda_\nu}\right) f_j\left(\mathbf{p}_{\mu_\nu}\right)\right)^{1-r_\nu} \left(f_i\left(\mathbf{p}_{\lambda_\nu+s_\nu}\right) f_j\left(\mathbf{p}_{\mu_\nu-s_\nu}\right)\right)^{r_\nu} \right\} \left| \frac{\mathbf{p}_{\alpha_\nu}}{m_i} - \frac{\mathbf{p}_{\beta_\nu}}{m_j} \right|. \tag{23}$$

Similarly, we obtain an expression for the value of the collision integral I_{ji} at some point $\mathbf{p}_{j_\gamma}$.

For the case of intracomponent collisions of molecules, when $i = j$, $I_{ij} = I_{ji}$, the formula for the collision integral is slightly modified, taking into account the symmetry of the collision integral,

$$I_{ii}(\mathbf{p}_\gamma) = B_{ii} \sum_{\nu=1}^{N_\nu} \{-(\delta_{\gamma,\alpha_\nu} + \delta_{\gamma,\beta_\nu}) + (1 - r_\nu)(\delta_{\gamma,\lambda_\nu} + \delta_{\gamma,\mu_\nu}) + r_\nu(\delta_{\gamma,\lambda_\nu+s_\nu} + \delta_{\gamma,\mu_\nu-s_\nu})\}\Delta_\nu^{ii}, \tag{24}$$

where

$$B_{ii} = \frac{\pi d_i^2 N_{0i} V_{0i}}{4N_\nu}$$

and

$$\Delta_\nu^{ii} = \left\{ f_i\left(\mathbf{p}_{\alpha_\nu}\right) f_i\left(\mathbf{p}_{\beta_\nu}\right) - \left(f_i\left(\mathbf{p}_{\lambda_\nu}\right) f_i\left(\mathbf{p}_{\mu_\nu}\right)\right)^{1-r_\nu} \left(f_i\left(\mathbf{p}_{\lambda_\nu+s_\nu}\right) f_i\left(\mathbf{p}_{\mu_\nu-s_\nu}\right)\right)^{r_\nu} \right\} \left| \frac{\mathbf{p}_{\alpha_\nu}}{m_i} - \frac{\mathbf{p}_{\beta_\nu}}{m_i} \right|. \tag{25}$$

If the molecular collision (defined by the node of the Korobov grid) gives a negative value of the distribution function at any of the 6 nodes of the momentum grid in (22) or (24), then it must be discarded. However, a significant number of discarded collisions can lead to a decrease in the simulation accuracy. In this work, we re-compute such collisions with the symmetric projection method (SPM), which was proposed in [Черемисин, 2006]. This method makes it possible to completely eliminate negative values of the distribution functions, but does not have the asymptotic property of the collision integral of the Maxwellian function being equal to zero.

The two-point conservative projection method described above is designed for single component gases and for gas mixtures with small or moderate ratios of molecular masses of mixture components [Anikin et al., 2012]. For mixtures with high ratios of molecular masses, a “multi-point” conservative projection method presented in [Anikin et al., 2014] is more efficient. In our work, we apply a five-point projection scheme to calculate the collision integral when the molecular mass ratio is greater than 2. In the five-point projection scheme, each momentum after collision is decomposed between 5 specially selected nodes, and the laws of conservation of energy, momentum and mass are fulfilled exactly.

Thus, in this paper, when the ratio of molecular masses of the components is no more than 2, the collision integrals on the right side of the relaxation equations (14) are evaluated using the formulas (19), (20), (24), (25), and the collision integrals in (16) are evaluated using the formulas (19), (20), (22), (23). In both cases, recalculation of collisions that give negative values of the distribution functions using the SPM is applied. When the ratio of molecular masses of the components is more than 2, to evaluate the collision integrals in (16), a five-point modification of the projection method is used. A detailed description of the CPM for a gas mixture is given in [Dodulad et al., 2016; Черемисин, 2015].

Statement of the problem

Consider a plane shock wave propagating in a gas mixture. We move to the frame of reference tied to the wave front. The X axis is aligned with the flow and is perpendicular to the shock front. Here and below, the physical quantities with subscripts 1 and 2 refer to the gas mixture ahead of and behind the shock wave, respectively. Macroscopic quantities of the gas mixture components ahead of and behind the shock wave are related by the Rankine – Hugoniot relations

$$\begin{gathered}\frac{n_2^i}{n_1^i} = \frac{u_1^i}{u_2^i} = \frac{u_1}{u_2} = \frac{(\gamma+1)M^2}{(\gamma-1)M^2+2}, \\ \frac{T_2^i}{T_1^i} = \frac{T_2}{T_1} = \frac{\left(2\gamma M^2-(\gamma-1)\right)\left((\gamma-1)M^2+2\right)}{(\gamma+1)^2M^2}.\end{gathered} \tag{26}$$

Here $n_{1,2}^i$, $u_{1,2}^i$ and $T_{1,2}^i$ are molecular densities, hydrodynamic velocities and temperatures of the i-th mixture component, respectively, $u_{1,2}$ and $T_{1,2}$ are velocities and temperatures of the entire mixture, γ is the adiabatic index, which for a monoatomic gas is equal to $\frac{5}{3}$, M is the Mach number, $u_1 = Mc_1$, where

$$c_1 = \sqrt{\gamma k_B T_1 \frac{\sum\limits_i n_1^i}{\sum\limits_i m^i n_1^i}}$$

is the speed of sound in the unperturbed (ahead of the shock wave) gas.

The problem is one-dimensional. The computational domain is $x \in (-L_1, L_2)$, where $L_1 > 0$ and $L_2 > 0$ are taken to be large enough so that the distribution functions $f^i(x = -L_1)$, $f^i(x = L_2)$ can be considered equilibrium. At the boundaries of the computational domain, the boundary conditions $f^i(x = -L_1) = f_1^i$, $f^i(x = L_2) = f_2^i$ are set. Here f_1^i and f_2^i are the distribution functions of the i-th mixture component ahead of and behind the shock front, respectively. The initial conditions are

$$f^i(x) = \begin{cases} f_1^i, & -L_1 \leqslant x \leqslant 0, \\ f_2^i, & 0 < x \leqslant L_2. \end{cases}$$

The shock wave structure is obtained in the course of the temporal evolution of the initial discontinuity at the point $x = 0$.

Numerical simulation parameters

Numerical simulation was performed using the previously developed and presented in [Sitnikov, Tcheremissine, 2021] simulation environment software, which allows one to study both steady and unsteady flows of gas mixtures in various flow regimes for arbitrary problem geometry. The computations were performed on a cluster architecture using MPI and OpenMP parallelization technologies [Quinn, 2004]. Due to symmetry, the solution of the advection equations was carried out only in $\frac{1}{4}$ of the momentum space. When solving the relaxation equations, the symmetry of the problem was also taken into account. Each collision, defined by a node of the Korobov integral grid, was symmetrically reflected along the Y and Z axes, due to which the effective size of the Korobov grid was 4 times higher. In this work, to improve the simulation accuracy, at the time step τ, we used the symmetric method of splitting by physical processes [Strang, 1968], in which the splitting operator has the form $A_{\tau/2}R_{\tau/2}A_{\tau/2}$, where $A_{\Delta t}$ is the operator of solving the system of advection equations (12), and $R_{\Delta t}$ is the operator of solving the complete system of relaxation equations (14) and (16) with a step Δt. The solution of the system of advection equations (12) is performed on a uniform spatial grid

using a difference TVD scheme, which has the second order of accuracy, both in time and in space, and has the property of monotonicity, on discrete values of the momentum.

To achieve high accuracy, computations were carried out at high sampling parameters. The computations were performed at two 12-core Intel Xeon E5 2680 v3, 2.50 GHz units. Through the Hyper-Threading, each task required 48 virtual cores. The acceleration of computations was at least 30.

The simulations were carried out for various values of the Mach number and ratios of molecular masses and densities of the mixture components:

1) $M = 3$, $\frac{m^\alpha}{m^\beta} = \frac{1}{2}$, $\frac{n_1^\alpha}{n_1^\beta} = 9$;

2) $M = 2$, $\frac{m^\alpha}{m^\beta} = \frac{1}{2}$, $\frac{n_1^\alpha}{n_1^\beta} = 1$;

3) $M = 2$, $\frac{m^\alpha}{m^\beta} = \frac{1}{4}$, $\frac{n_1^\alpha}{n_1^\beta} = 1$;

4) $M = 3$, $\frac{m^\alpha}{m^\beta} = \frac{1}{10}$, $\frac{n_1^\alpha}{n_1^\beta} = 1$.

Here and below, the superscripts α and β denote the components of the binary mixture. In the computations, $m^\beta = 1$, $n_1^\alpha + n_1^\beta = 1$, $d^\alpha = d^\beta = 1$, $T_1^\alpha = T_1^\beta = 1$, $m^\alpha < m^\beta$. The size of the computational domain was equal to $L_1 = L_2 = 10$, the space grid step $h_x = 0.1$, the cubature Korobov grid size was about $N_v = 10^6$, the momentum grid step $h_p^\beta = 0.4$, the radius of the momentum sphere $R^\beta = 15.8$. Thus, the number of grid points in momentum space was about $N_0^\beta = 3 \cdot 10^5$. The time step was equal to $h_t = 3 \cdot 10^{-2} \cdot \frac{m^\beta h_x}{R^\beta}$, while on the time interval (0; 0.1) the time step increased linearly from near zero to h_t, which somewhat increased the accuracy of computations. The simulations were performed on the time interval (0; 20), during which the temporal evolution of the initial discontinuity led to the formation of a stable shock wave structure. Accordingly, each task took about 10^5 steps by time. The radius of the sphere in momentum space R^α varied depending on the parameters of the mixture and the shock wave. The grid step in momentum space h_p^α was chosen in such a way as to preserve the number of grid points in momentum space, $N_0^\alpha \approx N_0^\beta = 3 \cdot 10^5$:

1) $R^\alpha = 15.8$, $h_p^\alpha = 0.4$ at $M = 3$, $\frac{m^\alpha}{m^\beta} = \frac{1}{2}$, $\frac{n_1^\alpha}{n_1^\beta} = 9$;

2) $R^\alpha = 15.8$, $h_p^\alpha = 0.4$ at $M = 2$, $\frac{m^\alpha}{m^\beta} = \frac{1}{2}$, $\frac{n_1^\alpha}{n_1^\beta} = 1$;

3) $R^\alpha = 7.9$, $h_p^\alpha = 0.2$ at $M = 2$, $\frac{m^\alpha}{m^\beta} = \frac{1}{4}$, $\frac{n_1^\alpha}{n_1^\beta} = 1$;

4) $R^\alpha = 5.925$, $h_p^\alpha = 0.15$ at $M = 3$, $\frac{m^\alpha}{m^\beta} = \frac{1}{10}$, $\frac{n_1^\alpha}{n_1^\beta} = 1$.

Results

Here and below, for convenience, the presented macroscopic quantities are normalized to the corresponding values at the boundaries of the computational domain

$$\widetilde{n} = \frac{n - n_1^\alpha - n_1^\beta}{n_2^\alpha + n_2^\beta - n_1^\alpha - n_1^\beta}, \quad \widetilde{u} = \frac{u - u_2}{u_1 - u_2}, \\ \widetilde{T} = \frac{T - T_1}{T_2 - T_1}, \quad \widetilde{T}^{\alpha,\beta} = \frac{T^{\alpha,\beta} - T_1}{T_2 - T_1}. \tag{27}$$

Figures 1–4 present the obtained distributions of n, u, T and $T^{\alpha,\beta}$ through the shock fronts for different values of the Mach number and the ratios of molecular masses and densities of the gas mixture components. At $M = 3$, $\frac{m^\alpha}{m^\beta} = \frac{1}{2}$, $\frac{n_1^\alpha}{n_1^\beta} = 9$, non-monotonic behavior of T^β is observed.

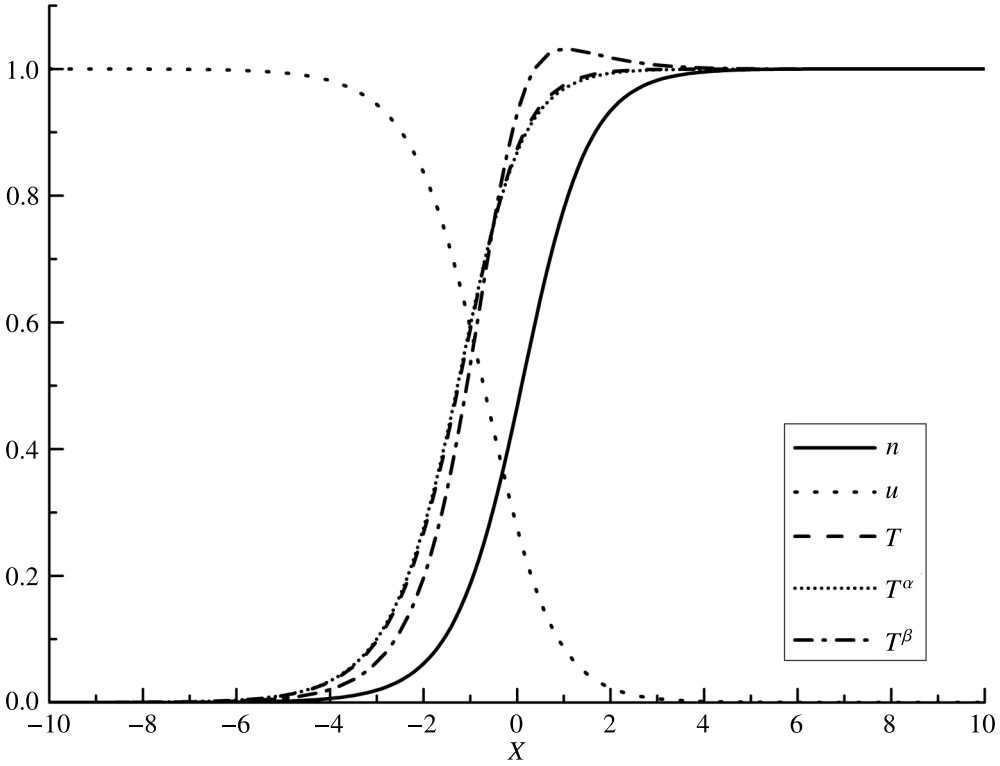

Figure 1. Distributions of the normalized values of molecular density n, hydrodynamic velocity u, temperature T of the mixture, and partial temperatures of the components $T^{\alpha,\beta}$ through the shock fronts at the Mach number and the ratios of molecular masses and densities of the components $M = 3$, $\frac{m^\alpha}{m^\beta} = \frac{1}{2}$, $\frac{n_1^\alpha}{n_1^\beta} = 9$. All quantities are dimensionless

Accuracy of the computations

The greatest influence on the accuracy of computations in the approach used is exerted by the time and spatial steps, the momentum step and the size of the cubature Korobov grid. To determine the magnitude of the numerical error, a series of computations were carried out for $M = 3$, $\frac{m^\alpha}{m^\beta} = \frac{1}{2}$, $\frac{n_1^\alpha}{n_1^\beta} = 9$, in which the above-mentioned simulation parameters were varied, and the results were compared with those obtained with the initial (unchanged) parameters. As the characteristics of the agreement between the results, we used the pointwise deviations of the molecular density and temperature of the mixture, as well as the inverse width of the shock wave, determined by the maximum slope of the molecular density profile:

$$\begin{gathered}\Delta_n(x) = |n'(x) - n(x)|, \quad \Delta_n = \max_{x\in(-L_1, L_2)} \Delta_n(x), \\ \Delta_T(x) = |T'(x) - T(x)|, \quad \Delta_T = \max_{x\in(-L_1, L_2)} \Delta_T(x), \\ \Delta_\delta = \frac{|\delta' - \delta|}{\delta}, \quad \delta = \max_{x\in(-L_1, L_2)} \left(\frac{dn(x)}{dx}\right), \quad \delta' = \max_{x\in(-L_1, L_2)} \left(\frac{dn'(x)}{dx}\right).\end{gathered} \tag{28}$$

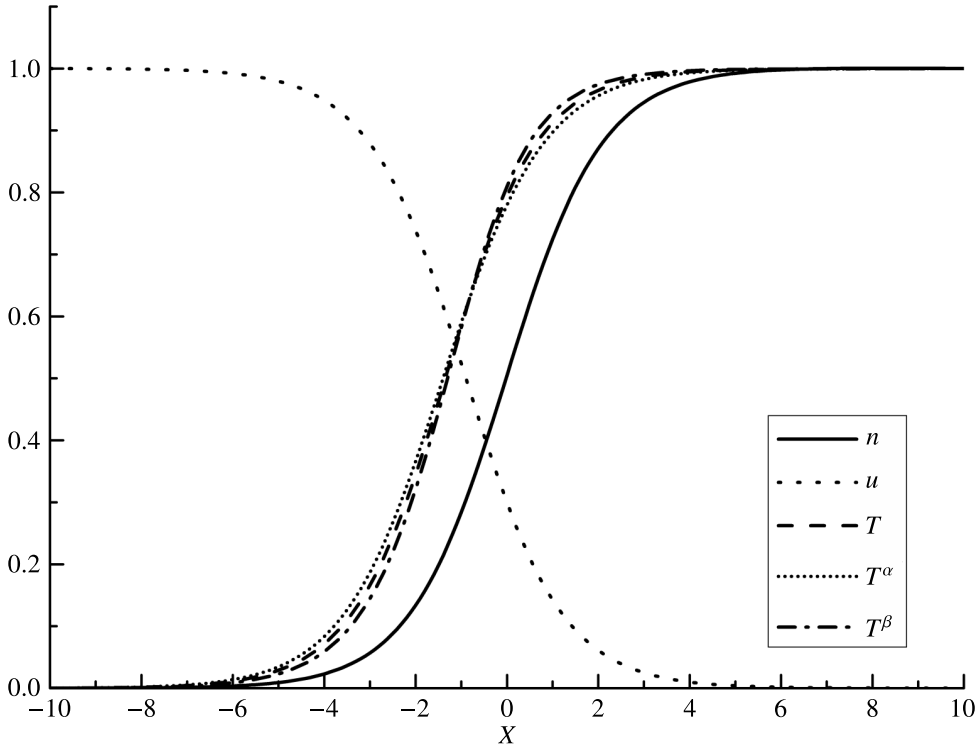

Figure 2. Distributions of the normalized values of molecular density n, hydrodynamic velocity u, temperature T of the mixture, and partial temperatures of the components $T^{\alpha,\beta}$ through the shock fronts at the Mach number and the ratios of molecular masses and densities of the components $M = 2$, $\frac{m^{\alpha}}{m^{\beta}} = \frac{1}{2}$, $\frac{n_1^{\alpha}}{n_1^{\beta}} = 1$

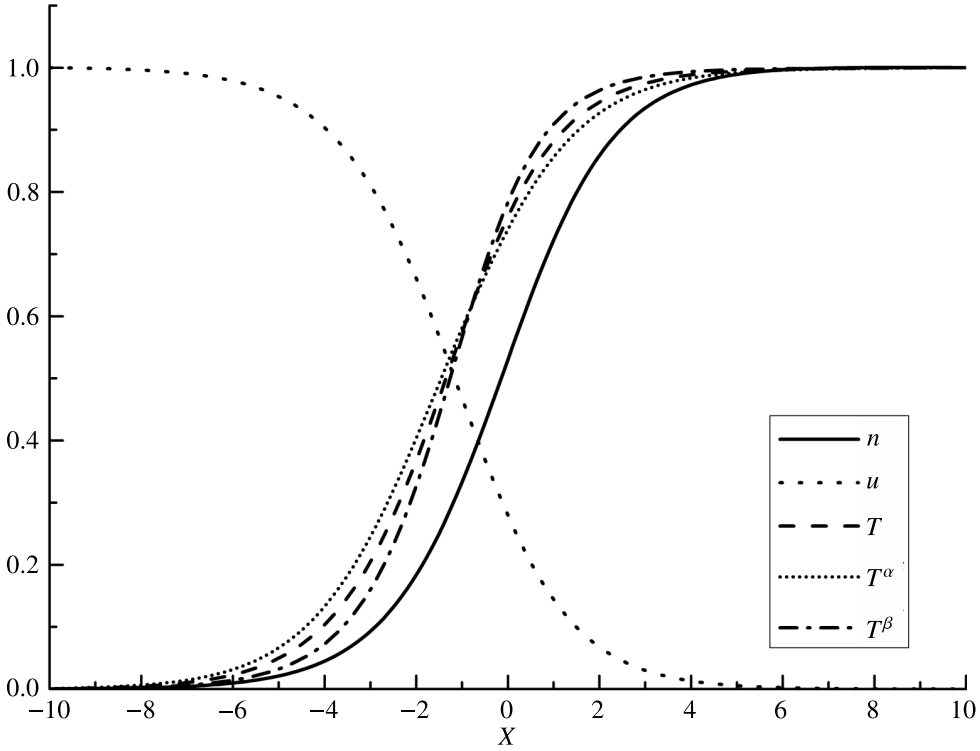

Figure 3. Distributions of the normalized values of molecular density n, hydrodynamic velocity u, temperature T of the mixture, and partial temperatures of the components $T^{\alpha,\beta}$ through the shock fronts at the Mach number and the ratios of molecular masses and densities of the components $M = 2$, $\frac{m^{\alpha}}{m^{\beta}} = \frac{1}{4}$, $\frac{n_1^{\alpha}}{n_1^{\beta}} = 1$

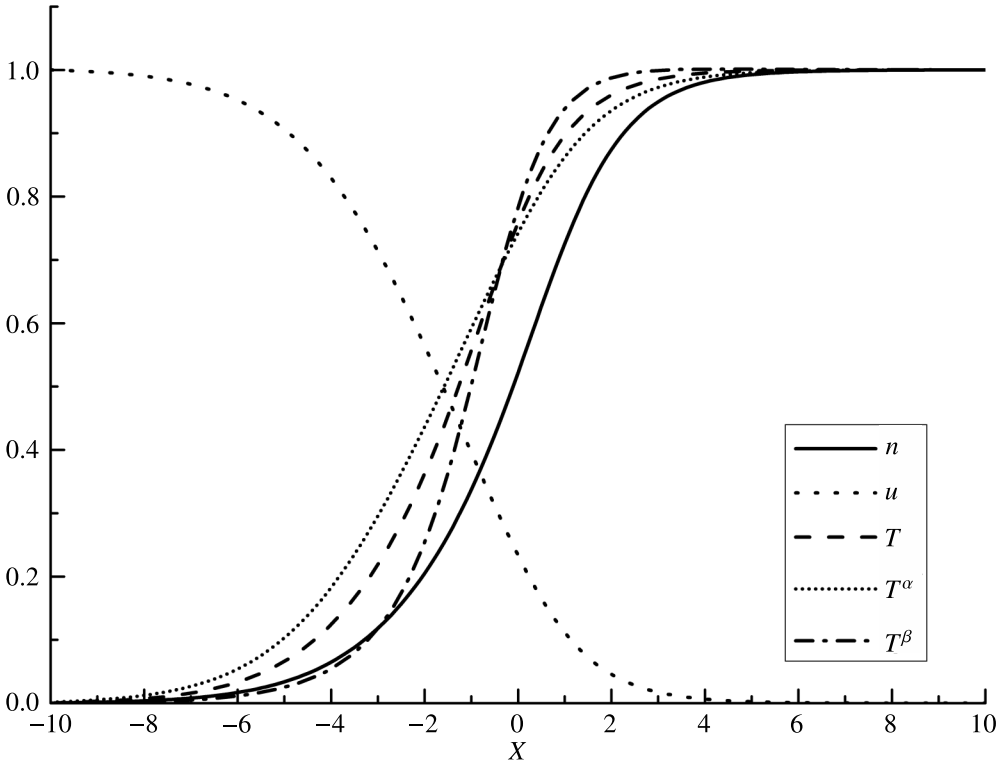

Figure 4. Distributions of the normalized values of molecular density n, hydrodynamic velocity u, temperature T of the mixture, and partial temperatures of the components $T^{\alpha,\beta}$ through the shock fronts at the Mach number and the ratios of molecular masses and densities of the components $M = 3$, $\frac{m^\alpha}{m^\beta} = \frac{1}{10}$, $\frac{n_1^\alpha}{n_1^\beta} = 1$

Here all the macroscopic characteristics are given in its normalized form (27). The values with the prime symbol are obtained for the variation of some of the numerical simulation parameters, and the unprimed values are computed for the original parameters. The inverse shock front width is defined as

$$\delta = \frac{\lambda_1}{n_2 - n_1} \max_{x\in(-L_1, L_2)} \left(\frac{dn(x)}{dx}\right) \approx \frac{1}{n_2 - n_1} \max_{x\in(-L_1, L_2)} \left(\frac{dn(x)}{dx}\right) = \max_{x\in(-L_1, L_2)} \left(\frac{dn(x)}{dx}\right), \tag{29}$$

where λ_1 is the mean free path in an unperturbed (ahead of the shock wave) gas, which in dimensionless units is equal to 1.

The corresponding numerical errors are defined as

$$\varepsilon_n = \sum_k \lim_{a_k\to 0} \Delta_n, \quad \varepsilon_T = \sum_k \lim_{a_k\to 0} \Delta_T, \quad \varepsilon_\delta = \sum_k \lim_{a_k\to 0} \Delta_\delta, \tag{30}$$

where a_k is one of the $k = 4$ simulation parameters: the time step $a_1 = h_t$, the squared space step $a_2 = h_x^2$, the squared momentum step $a_3 = h_p^2$ and the inverse size of the Korobov grid $a_4 = N_\nu^{-1}$. The numerical error of the obtained results is defined as follows

$$\varepsilon_{num} = \max(\varepsilon_n, \varepsilon_T). \tag{31}$$

We carried out test computations with the following parameter variations: the time step $h_t'^{(1)} = 2h_t$, $h_t'^{(2)} = 3h_t$, $h_t'^{(3)} = 4h_t$ and $h_t'^{(4)} = 5h_t$; the space step $h_x'^{(1)} = 1.5h_x$, $h_x'^{(2)} = 1.9h_x$, $h_x'^{(3)} = 2.2h_x$ and $h_x'^{(4)} = 2.5h_x$; the momentum step $h_p'^{(1)} = 1.325h_p$, $h_p'^{(2)} = 1.575h_p$, $h_p'^{(3)} = 1.8h_p$ and $h_p'^{(4)} = 2h_p$; the size of the Korobov grid $N_\nu'^{(1)} = 0.5N_\nu$, $N_\nu'^{(2)} = 0.3N_\nu$, $N_\nu'^{(3)} = 0.2N_\nu$ and $N_\nu'^{(4)} = 0.1N_\nu$. When varying the spatial step, the values of the macroscopic parameters at the missing spatial points

were determined using cubic spline interpolation. Figure 5 presents the obtained results for $\delta'(a_k)$. For all a_k, the values computed in a series of runs are reasonably approximated by linear dependencies, which is consistent with the theoretical orders of convergence of the numerical error on the simulation parameters.

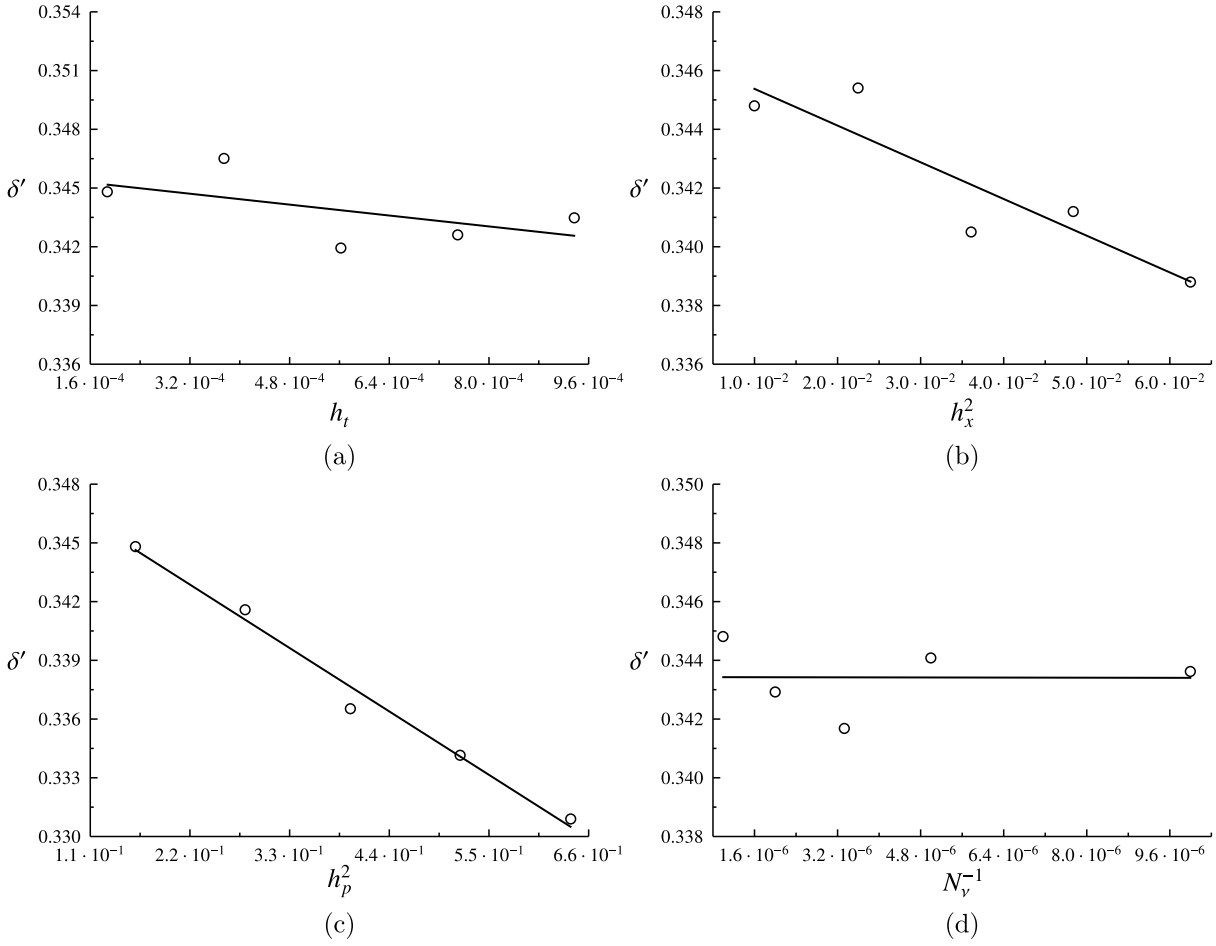

Figure 5. Numerical results for the inverse shock front width $\delta'(a_k)$ obtained by varying the parameter a_k, where the variation parameter is (a) the time step $a_1 = h_t$, (b) the squared space step $a_2 = h_x^2$, (c) the squared momentum step $a_3 = h_p^2$, (d) the inverse Korobov grid size $a_4 = N_\nu^{-1}$. All quantities are dimensionless

In accordance with the corresponding definitions, the following values of the numerical error were obtained:

$$\varepsilon_n = \sum_k \lim_{a_k \to 0} \widetilde{\Delta}_n(a_k) \approx 9.0 \cdot 10^{-3},$$

$$\varepsilon_T = \sum_k \lim_{a_k \to 0} \widetilde{\Delta}_T(a_k) \approx 1.1 \cdot 10^{-2},$$

$$\varepsilon_\delta = \sum_k \lim_{a_k \to 0} \frac{|\widetilde{\delta'}(a_k) - \delta|}{\delta} \approx 2.5 \cdot 10^{-2}.$$

Here $\widetilde{\Delta}_n(a_k)$, $\widetilde{\Delta}_T(a_k)$ and $\widetilde{\delta'}(a_k)$ are the linear approximations of the corresponding values obtained in a series of runs. According to the given estimates, the magnitude of the numerical error of the simulation results was $\varepsilon_{num} = \max(\varepsilon_n, \varepsilon_T) \approx 1\,\%$. The higher value of the error in the width of the

shock wave front is due to the fact that the evaluation is carried out based on the derivative of the distribution of the mixture molecular density.

Comparison of the results obtained using the two-point and five-point projection methods

We studied the influence of the projection scheme on the simulation results. As a metric for the agreement between the results, we used the modulus of the difference in the normalized molecular densities of the mixture obtained for $M = 2$, $\frac{m^\alpha}{m^\beta} = \frac{1}{2}$, $\frac{n_1^\alpha}{n_1^\beta} = 1$ using the two-point and five-point projection methods

$$\Delta_n(x) = |n_{2p}(x) - n_{5p}(x)|. \tag{32}$$

The maximum value of the deviation of the results obtained with different methods was $\varepsilon_{method} = \max\limits_{x\in(-L_1, L_2)} \Delta_n(x) = 4.1 \cdot 10^{-3} < \varepsilon_{num}$. Thus, the projection scheme used does not have a significant impact on the simulation results.

Comparison of the obtained results with the available computation data

Figure 6 compares the results obtained for $M = 3$, $\frac{m^\alpha}{m^\beta} = \frac{1}{2}$, $\frac{n_1^\alpha}{n_1^\beta} = 9$ and $M = 2$, $\frac{m^\alpha}{m^\beta} = \frac{1}{4}$, $\frac{n_1^\alpha}{n_1^\beta} = 1$ with the data presented in [Kosuge, Aoki, Takata, 2001]. The solid line shows the graphs of normalized molecular densities of the mixture computed in this work. Data from [Kosuge, Aoki, Takata, 2001] are indicated by crosses.

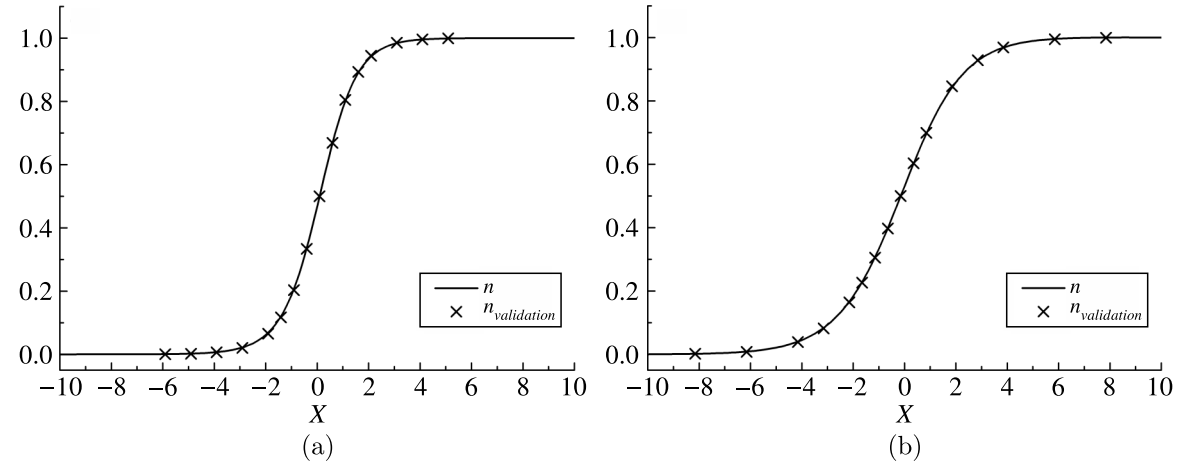

Figure 6. Comparison of the obtained distributions of the normalized molecular density of the mixture n through the shock fronts with the numerical data $n_{validation}$ presented in [Kosuge, Aoki, Takata, 2001] at the Mach number and the ratios of molecular masses and densities of the components: (a) $M = 3$, $\frac{m^\alpha}{m^\beta} = \frac{1}{2}$, $\frac{n_1^\alpha}{n_1^\beta} = 9$, (b) $M = 2$, $\frac{m^\alpha}{m^\beta} = \frac{1}{4}$, $\frac{n_1^\alpha}{n_1^\beta} = 1$. All quantities are dimensionless

As a metric for the agreement between the results, we used the modulus of the difference in the normalized molecular densities of the mixture obtained in this work and presented in [Kosuge, Aoki, Takata, 2001]:

$$\Delta_n(x) = |n(x) - n_{validation}(x)|. \tag{33}$$

The maximum value of the deviation of the molecular densities was $\varepsilon_{validation} = \max\limits_{x\in(-L_1, L_2)} \Delta_n(x) = 3.7 \cdot 10^{-3} < \varepsilon_{num}$ at $M = 3$, $\frac{m^\alpha}{m^\beta} = \frac{1}{2}$, $\frac{n_1^\alpha}{n_1^\beta} = 9$ and $\varepsilon_{validation} = \max\limits_{x\in(-L_1, L_2)} \Delta_n(x) = 3.4 \cdot 10^{-3} < \varepsilon_{num}$ at $M = 2$, $\frac{m^\alpha}{m^\beta} = \frac{1}{4}$, $\frac{n_1^\alpha}{n_1^\beta} = 1$, which demonstrates good agreement between the obtained results and the given computation data.

Conclusion

The structure of a shock wave in a binary gas mixture is studied based on direct solution of the Boltzmann kinetic equation. The applied numerical methods are described in detail. The computation parameters are provided to reproduce the results. The distributions of macroscopic quantities of the mixture components through the shock wave fronts are obtained for various Mach numbers and the ratios of molecular masses with a fixed accuracy controlled by the simulation parameters. The numerical error was no more than 1 % for local values of molecular density and temperature of the mixture and 3 % for the shock front width. The results presented in this paper are of theoretical significance, and can serve as a test computation, since they are obtained using the exact Boltzmann equation.

Special attention is paid to the verification of the obtained results. A thorough analysis of the simulation accuracy was carried out. The computed results for the shock front structure were compared with those given in [Kosuge, Aoki, Takata, 2001], as well as the results obtained using the two-point method were compared with those obtained with the five-point one. The achieved numerical simulation accuracy and good agreement between all the results approve the applicability of the proposed approach for modeling shock waves in gas mixtures.

References

Коган М. Н. Динамика разреженного газа. — Наука, 1967.
Kogan M. N. Dinamika razrezhennogo gaza [Rarefied gas dynamics]. — Nauka, 1967 (in Russian).

Коробов Н. М. Тригонометрические суммы и их приложения. — Наука, 1989.
Korobov N. M. Trigonometricheskie summy i ikh prilozheniya [Trigonometric sums and their applications]. — Nauka, 1989 (in Russian).

Черемисин Ф. Г. Введение в консервативный проекционный метод вычисления интеграла столкновений и метод решения уравнения Больцмана. — МФТИ, 2015.
Tcheremissine F. G. Vvedenie v konservativnyi proektsionnyi metod vychisleniya integrala stolknovenii i metod resheniya uravneniya Bol'tsmana [Introduction to the conservative projection method for calculating the collision integral and the method for solving the Boltzmann equation]. — MFTI, 2015 (in Russian).

Черемисин Ф. Г. Консервативный метод вычисления интеграла столкновений Больцмана // Доклады Академии наук. Сер. Физика. — 1997. — Т. 21. — С. 197–203.
Tcheremissine F. G. Conservative method for calculating the Boltzmann collision integral // Doklady Physics. — 1997. — Vol. 42. — P. 607–610. (Original Russian paper: *Cheremisin F. G.* Konservativnyi metod vychisleniya integrala stolknovenii Bol'tsmana // Doklady Akademii nauk. Ser. Fizika. — 1997. — Vol. 21. — P. 197–203.)

Черемисин Ф. Г. Решение кинетического уравнения Больцмана для высокоскоростных течений // Журнал вычислительной математики и математической физики. — 2006. — Т. 46, № 2. — С. 329–343.
Tcheremissine F. G. Solution to the Boltzmann kinetic equation for high-speed flows // Computational Mathematics and Mathematical Physics. — 2006. — Vol. 46, No. 2. — P. 315–329. (Original Russian paper: *Cheremisin F. G.* Reshenie kineticheskogo uravneniya Bol'tsmana dlya vysokoskorostnykh techenii // Zhurnal vychislitel'noi matematiki i matematicheskoi fiziki. — 2006. — Vol. 46, No. 2. — P. 329–343.)

Черемисин Ф. Г. Решение уравнения Больцмана при переходе к гидродинамическому режиму течения // Доклады Академии наук. Сер. Физика. — 2000. — Т. 373, № 4. — С. 483–486.

Tcheremissine F. G. Solving the boltzmann equation in the case of passing to the hydrodynamic flow regime // Doklady Physics. — 2000. — Vol. 45, No. 8. — P. 401–404. (Original Russian paper: *Cheremisin F. G.* Reshenie uravneniya Bol'tsmana pri perekhode k gidrodinamicheskomu rezhimu techeniya // Doklady Akademii nauk. Ser. Fizika. — 2000. — Vol. 373, No. 4. — P. 483–486.)

Anikin Yu., Dodulad O. I., Kloss Yu., Martynov D. V., Shuvalov P. V., Tcheremissine F. G. Development of applied software for analysis of gas flows in vacuum devices // Vacuum. — 2012. — Vol. 86. — P. 1770–1777.

Anikin Yu. A., Dodulad O. I., Kloss Yu. Yu., Tcheremissine F. G. Method of calculating the collision integral and solution of the Boltzmann kinetic equation for simple gases, gas mixtures and gases with rotational degrees of freedom // International Journal of Computer Mathematics. — 2014. — Vol. 92. — P. 1775–1789.

Aristov V. V., Cheremisin F. G. The conservative splitting method for solving Boltzmann's equation // USSR Computational Mathematics and Mathematical Physics. — 1980. — Vol. 20. — P. 208–225.

Bird G. A. The DSMC method. — Create Space Independent Publishing Platform, 2013.

Cao Z., White C. M., Kontis K. Numerical investigation of rarefied vortex loop formation due to shock wave diffraction with the use of rorticity // Physics of Fluids. — 2021. — Vol. 33.

Dodulad O. I., Kloss Y. Y., Potapov A. P., Tcheremissine F. G., Shuvalov P. V. Simulation of rarefied gas flows on the basis of the Boltzmann kinetic equation solved by applying a conservative projection method // Computational Mathematics and Mathematical Physics. — 2016. — Vol. 56. — P. 996–1011.

Dodulad O. I., Tcheremissine F. G. Computation of a shock wave structure in monatomic gas with accuracy control // Computational Mathematics and Mathematical Physics. — 2013. — Vol. 53. — P. 827–844.

Gospodinov P., Roussinov V., Dankov D. Thermoacoustic waves in a cylindrical Couette rarefied gas flow // AIP Conference Proceedings. — 2014. — Vol. 1629.

Hirschfelder J. O., Curtiss C. F., Bird R. B. Molecular theory of gases and liquids. — John Wiley & Sons, Inc., 1954.

Kloss Y. Y., Ryabchenkov V. V., Tcheremissine F. G., Shuvalov P. V. Interaction of a shock wave with a boundary layer in a micro channel // Mathematical Models and Computer Simulations. — 2011. — Vol. 3.

Kosuge S., Aoki K., Takata S. Shock-wave structure for a binary gas mixture: finite-difference analysis of the Boltzmann equation for hard-sphere molecules // European Journal of Mechanics B-fluids. — 2001. — Vol. 20. — P. 87–126.

Quinn M. J. Parallel programming in C with MPI and OpenMP. — McGraw-Hill Science, Engineering & Mathematics, 2004.

Raines A. Study of a shock wave structure in gas mixtures on the basis of the Boltzmann equation // European Journal of Mechanics B-fluids. — 2002. — Vol. 21. — P. 599–610.

Sharipov F., Dias F. C. Ab initio simulation of planar shock waves // Computers & Fluids. — 2017. — Vol. 150. — P. 115–122.

Sharipov F., Seleznev V. Data on internal rarefied gas flows // J. Phys. Chem. Ref. Data. — 1998. — Vol. 27. — P. 657–706.

Sitnikov S. S., Tcheremissine F. G. Simulation of mixture components separation in a rarefied argon-neon jet on the basis of direct solution of the Boltzmann kinetic equation // Journal of Computational Science. — 2021. — Vol. 55. — 101467.

Strang G. On the construction and comparison of difference schemes // SIAM Journal on Numerical Analysis. — 1968. — Vol. 5. — P. 506–517.

Wu Z., Xu Y., Wang W., Hu R. Review of shock wave detection method in CFD post-processing // Chinese Journal of Aeronautics. — 2013. — Vol. 26. — P. 501–513.

Xu K. A unified computational fluid dynamics framework from rarefied to continuum regimes. — Cambridge University Press, 2021.